Transition-State Theory Model for the Diffusion Coefficients of Small Penetrants in Glassy Polymers

Angus A. Gray-Weale, Richard H. Henchman,† and Robert G. Gilbert*

School of Chemistry, Sydney University, Sydney, NSW 2006, Australia

Michael L. Greenfield‡ and Doros N. Theodorou§

Department of Chemical Engineering, University of California, Berkeley, California 94720

Received March 14, 1997; Revised Manuscript Received August 4, 1997⊗

ABSTRACT: Previous molecular dynamics simulations have shown that the diffusion of a penetrant in a glassy polymer involves occasional jumps between cavities through the opening of a "neck", and thus, because this is a rare event, the diffusion coefficient can be estimated using transition-state theory. We treat this process as a unimolecular rearrangement and develop semiempirical means of estimating the activation energy, frequency factor and jump length. The activation energy is obtained by treating the polymer as a continuous solid and calculating the energy required to expand a neck in that continuum. The model for the frequency factor uses the result from simulations that the distribution of frequencies of the modes in the transition is very similar to that distribution for the reactant state. The frequency factor is estimated by considering only the motion of the penetrant. These motions are treated as harmonic oscillators. The jump length is obtained from simple geometric considerations of the polymer chain. The parameters are readily evaluated from bulk properties of the polymer such as the isothermal compressibility. The model reproduces experimental trends semiquantitatively and could be used to interpolate and extrapolate experimental diffusion data.

Introduction

The diffusion of small species in a glassy polymer has both practical and theoretical importance. Diffusion controls quantities such as the permeability of a polymer to gases, membrane selectivity,[1] the molecular weight distribution of a polymer, polymerization rates at high conversion, and the control of residual monomer.[2] Our objective in this paper is to use the simulation data obtained by two of the present authors[3−6] to develop a simple analytic model for diffusion in glassy polymers, so that diffusion coefficients may be predicted without time-consuming computer simulations.

In rubbery polymers, where the polymer's mobility is high, diffusion is assisted by the polymer's motions, which push the penetrant along.[7] Near the glass transition, the polymer motions become restricted, and the unoccupied volume becomes fixed.[3,8−11] In order for penetrants to diffuse in such a glassy system, they must jump from cavity to cavity. There is likely to be a significant activation energy[12−14] for these jumps, and indeed such barriers have been observed in molecular dynamics simulations.[15−17] The change in temperature dependence of the diffusion coefficient at the glass transition[18] is further evidence for the change in the mechanism of diffusion.

When the motion is dominated by rare activated events, transition state theory applies.[19] The basic premise is that the penetrant spends most of its time rattling around in a cavity. Occasionally, a neck to a neighboring cavity opens, and the penetrant may jump through it. While such a situation may lead to non-Brownian behavior,[20−23] we follow most workers in assuming that the bulk diffusion coefficient may be found from the mean-squared displacement ($\langle r^2(t)\rangle = 6Dt$) relation. Examination of non-Brownian behavior will be the subject of future work.

Using the simulation data,[3−6] we aim to develop an intuitive understanding of the frequency factors and energies for the diffusive jumps. Using approximate models for the Hamiltonians of the reactant and transition states, we find ways of estimating these quantities from known physical properties (such as the bulk Young's modulus), without the use of large-scale computer simulations. A similar semiempirical approach is used routinely to predict and interpret the rate coefficients of unimolecular reactions in the gas phase.[19]

Previous models have either been computationally intensive or have been based on assumptions about the physical nature of the system which were not tested against simulation data. The dual-mode sorption model[24] assumes that penetrants can exist in either of two types of environment, each with different diffusive properties. Free-volume models[25−31] assume that the probability of a diffusive jump is proportional to the probability of a critical amount of free volume accumulating adjacent to the penetrant. Finally there are the "molecular" models[32,33] which calculate the energy for a simplified polymer motion: for example, Pace and Datyner[34−36] assumed Arrhenius behavior for the rate coefficient of an idealized diffusive process.

Summary of Transition-State Simulations

Transition-state theory (TST) provides an approximate way to calculate the rate coefficient, k_{jump}, of each possible jump from cavity to cavity in a polymer microstructure. The movement of the penetrant from the reactant state cavity through the transition state neck to a neighboring cavity is a unimolecular rearrangement.[19] The rate coefficient for the jump is obtained from the TST formula:

* To whom correspondence should be addressed.
† Present address: Chemistry Department, The University of Southampton, Highfield. Southampton SO17 1BJ, U.K.
‡ Present address: Ford Research Laboratory, Ford Motor Company, P.O. Box 2053, Mail Drop 3083/SRL, Dearborn, MI 48121-2053.
§ Present address: Department of Chemical Engineering, University of Patras, Patras, GR-26500, Greece.
⊗ Abstract published in *Advance ACS Abstracts,* November 1, 1997.

S0024-9297(97)00349-5 CCC: $14.00

$$k_{\text{jump}} = \frac{k_B T Q^{\dagger}}{h \; Q} \exp(-E_0/k_B T) \qquad (1)$$

where $Q^{\dagger}$ and Q are the partition functions of transition state and reactant, respectively, and E_0 is the difference in energy between the reactant minimum and the transition-state saddle point.

The first attempt at the TST approach for diffusion in polymers was by Jagodic *et al.* in 1973.[37] The approach has been developed by Gusev and Suter and by Theodorou and co-workers, among others.[3−5,38−40] The first application of TST to glassy polymers by Gusev *et al.* allowed only the penetrant's three translational degrees of freedom to vary, leaving the polymer fixed.[38] While diffusion coefficients obtained for very small penetrants such as helium compared reasonably with experiment, coefficients for larger penetrants such as O_2 were orders of magnitude too small. The reason for the error is probably that the large penetrants depend on polymer motions to allow them through, so holding the polymer fixed only works for small penetrants. In order to give the polymer some flexibility, Gusev and Suter added elastic thermal motion to the polymer during the stochastic simulations. Short molecular dynamics runs were used to characterize and quantify these motions. Diffusion coefficients so obtained agreed with experiment within an order of magnitude.

To find the lowest energy path for a penetrant moving between two cavities, Greenfield and Theodorou[3−6] explicitly included polymer degrees of freedom in the TST calculation, thus allowing the polymer to assist in forming a neck for the penetrant to squeeze through to the next cavity. They located cavities as clusters of local energy minima in a Lennard−Jones model of a polymer, found saddle points,[41] and tracked necks by following the reaction coordinate in the usual "steepest descent" manner, starting from the saddle point (see Figure 1). This gives the required properties of the transition state. These simulation data, comprising reactant minima, transition-state jump rate coefficients, and jump lengths, are the ones used in the present paper as a guide.

Such TST calculations can then be used in a stochastic simulation[42] to produce a macroscopic diffusion coefficient.[38] The advantage of stochastic simulations is that very long times can be simulated, since the basic time unit is now of order 1 ps rather than 1 fs for molecular dynamics. Molecular dynamics simulations[7,11,15−17,43−60] are useful for calculating diffusion coefficients in rubbery polymers but do not sample large enough time scales to provide reliable information about glassy diffusion. At the time of writing, only a few stochastic simulations using TST have been applied to glassy diffusion.[39,40] The difficulty lies in the extremely broad distribution of jumps, which requires a large simulation box so there are enough jumps available to sample the whole distribution. If the box is too small, false Brownian diffusion is observed, since the use of periodic boundary conditions enforces an artificial crystallinity on the polymer. It has been found[38] that when penetrants on average have diffused the length of the box, an artificial linear relationship between $\langle r(t)^2 \rangle$ and t sets in at short times. The box should be large enough so that there is no change in this relationship when penetrants have diffused the length of the box.

The system simulated by Greenfield and Theodorou was glassy atactic polypropylene at 233 K with an empirical force field. A polymer matrix consisting of three polymer chains, each of 50 monomer units, was

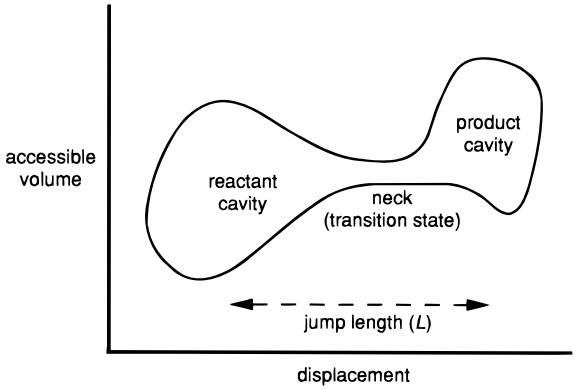

Figure 1. Illustration of the accessible volume of a penetrant as it jumps, via a neck, from one cavity to another.

generated by the rotational isomeric state model modified to allow for nonbonded interactions[61] and then energy-minimized by molecular mechanics. Transition states and reaction coordinates were found and tracked in structures that resided in local potential energy minima. The methane penetrant was taken as spherically symmetric, and the united-atoms approximation was used for the penetrant and methyl groups on the polymer chains. As well as the penetrant's translational degrees of freedom, torsion and bond angles associated with polymer atoms in a sphere of radius about 9 Å surrounding the penetrant were made flexible. As the penetrant moved, this set was continually updated so that it always surrounded the penetrant. All other degrees of freedom including all bond stretches were considered infinitely stiff.[62]

In order to find reactant cavities and connecting transition-state necks, a geometric analysis of volume unoccupied by the polymer was performed.[3] This eliminates large parts of the potential energy surface in which to search for true minima and transition states. For this analysis, Greenfield and Theodorou treated polymer and penetrant as hard spheres with radii $r_p = 2^{1/6}(\sigma/2)$, where σ is the Lennard−Jones diameter of the particular atom. Accessible volume for a penetrant of radius r_p was defined as volume in the polymer matrix traced out by the penetrant's center for all the regions in which the penetrant can fit. In other words, if the radius of the polymer atoms is increased by r_p, the space left over is termed accessible volume. Clusters of volume left over for $r_p = 2.09$ Å correspond to accessible volume for methane. Unoccupied volume is just accessible volume for a penetrant with zero radius. Greenfield and Theodorou used Delaunay tessellation for volume calculations,[63,64] in which space is broken up into tetrahedra with vertices at the polymer atoms. Accessible volume is then found by "clustering" these tetrahedra together. Possible reactant and product cavities are not restricted to these structures, since polymer rearrangement and partial squashing of the penetrant, not considered in this hard sphere treatment, would allow methane molecules to fit into smaller cavities, and thus possible reactant and product cavities are taken as clusters for $r_p = 1.3$ Å. Possible necks connecting them were taken from the accessible volume clusters for $r_p = 0.6$ Å. After the reactant minimum and transition state were located, normal mode analysis was used to find the harmonic frequencies of reactant and transition state. The classical transition-state rate coefficient was then found by the usual method.[19]

Table 1. Parameters for Forward and Backward Jumps of Eight Jumps[a]

jump no.	E_0, kJ mol^{-1}	E_{def}, kJ mol^{-1}	E_{LJ}, kJ mol^{-1}	$Q^\dagger/Q$	k, 10^6 s^{-1}	L, Å
1 forward	18.1	6.2	11.9	0.18	77	7.6
1 backward	23.5	6.3	17.2	0.36	9.3	
2 forward	11.3	9.6	1.7	0.024	336	5.9
2 backward	19.1	10.7	8.4	0.20	52	
3 forward	32.7	26.6	6.1	0.12	0.0027	5.4
3 backward	24.3	18.5	5.7	0.79	14	
4 forward	41.0	26.5	14.3	0.0056	2×10^{-5}	7.6
4 backward	45.3	25.3	20.0	0.0074	3×10^{-5}	
5 forward	19.8	8.3	11.5	0.0020	0.37	6.8
5 backward	12.8	6.1	6.7	0.0001	0.63	
6 forward	27.1	21.7	5.4	0.050	0.20	3.2
6 backward	16.6	12.5	4.1	0.13	115	
7 forward	19.4	19.1	0.3	0.050	13	3.0
7 backward	14.7	14.0	0.3	0.024	58	
8 forward	22.6	13.9	8.8	0.076	3.0	4.6
8 backward	33.3	22.0	11.4	0.070	0.011	

[a] E_{def} is the energy for the polymer to form a neck, E_{LJ} is the energy for penetrant to squeeze through the neck, and E_0 is the total.

The jump length is the displacement between reactant and product minima (Figure 1). However, reactant and product cavities consist of many minima separated by energy barriers small relative to k_BT, allowing penetrants ready access to the whole cavity. Thus the effective jump length was taken as the displacement between the centers of reactant and product cavities.

Details of simulations, both forward and backward, through eight necks, are summarized in Table 1, which shows rate coefficients k_{jump} varying from 10^1 to 10^8 s^{-1}, energy differences E_0 from 11 to 45 kJ mol^{-1}, and jump lengths L from 3 to 8 Å. More extensive results are also available.[65] The simulation data were also used to break the critical energy into two components: E_{def} is the energy for the polymer to form a neck, and E_{LJ} is the energy for penetrant to squeeze through the Lennard−Jones potentials of the neck. These results will be used in the development of our model. These eight jumps were chosen at random and hopefully represent a typical collection of jumps in the polymer microstructure. While there are not enough jumps to ascertain various quantities on a statistical basis, it is hoped that eight are enough to show what features of the jumps are important.

Model Development

In order to obtain a diffusion coefficient, the penetrant's extremely complex motion has to be simplified. In glassy systems the jump is the rate-determining step. All other motion is irrelevant to diffusion, except over very short time scales. There are no other competing diffusion mechanisms such as unoccupied volume redistributions sweeping penetrants along as in rubbery polymers, since the polymer matrix and cavities are mostly fixed in space. It is assumed here that penetrants, while trapped in cavities, are unable to move a net displacement within the cavity which is significant with respect to the jump length. The rate-determining step is *not* the time taken to jump from one cavity to another but instead the time spent rattling around in the cavity before the jump. From the simulations, the jump itself typically lasts ~1 ps,[43] while simulated waiting times were ~100 ps[43] to 1 ns[53] near T_g and significantly longer well below T_g.

The only motions that greatly affect the frequency factor are those of low frequency and those that are significantly different in reactant and transition state. The critical energy is just the difference between the energy minima of the reactant and transition state, so it does not depend on the details of the motion.

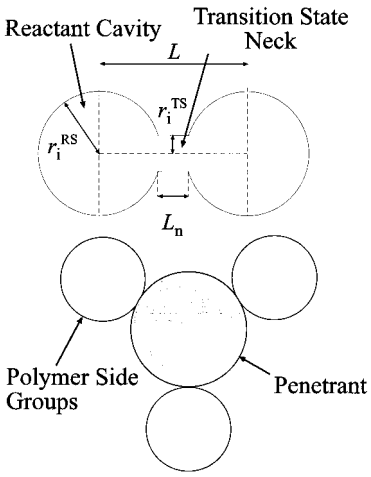

Figure 2. Diagram of the geometry of the model. The upper diagram shows the dimensions of the reactant cavity and the transition state neck. The lower diagram shows the trigonal arrangement of the side groups around the penetrant in the transition state. The reactant state has four of the side groups arranged tetrahedrally.

Once we have a model for the rate constant, k_{jump}, and length, L, of the typical jump, we can find the diffusion coefficient assuming only typical jumps take place:

$$D = {}^1/_6 k_{jump} L^2 \tag{2}$$

Model for Geometry. The geometry of our model is shown in Figure 2. When a penetrant jumps from one cavity to another cavity, it jumps through a neck past some part of a polymer chain. The results from the transition state theory simulations indicate that most jumps go past the polymer's side groups. The neck's length is therefore taken as the width of the side group. In the case of the simulations on polypropylene, these are methyl groups. Since the jump length is measured from the center of the reactant cavity to that of the product cavity, the size of the reactant cavity also needs to be included in the jump length, as can be seen in Figure 2. We therefore take the jump length as the size of the cavity added to the Lennard−Jones diameter of the polymer's side group:

$$L = L_n + 2r_i^{RS} \tag{3}$$

where L_n and r_i^{RS} are illustrated in Figure 2, and

$$L_n = \sigma(\text{side group}) \tag{4}$$

The transition state neck is assumed to be made up of three side groups, arranged trigonally.

The simulations show that the most common type of polymer "atoms" around penetrants in reactant cavities are also side groups, and so the cavity is assumed to comprise the penetrant surrounded by four side groups located at the corners of a tetrahedron. Arizzi[66] also took the Delaunay tetrahedra defined by the polymer configuration, found the potential energy minimum in each one with respect to a spherical penetrant in a fixed polymer, and found a transition state on each tetrahedron's face; this is a geometry similar to the one given here.

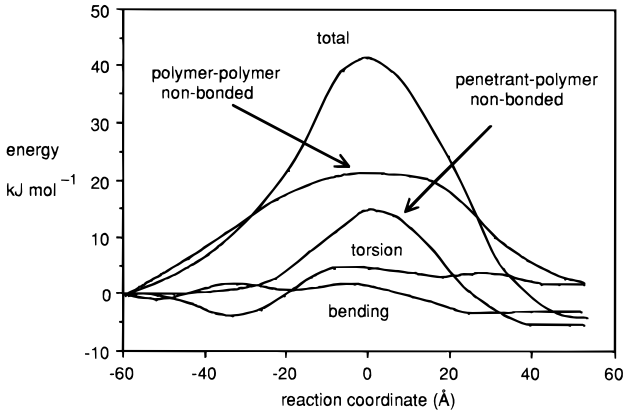

Figure 3. Energy profile along the reaction coordinate for jump number 4 in the simulations (see Table 1). Shown also are the changes in the individual energy contributions (bends, torsions, polymer-polymer nonbonded, penetrant-polymer nonbonded).

When one is calculating the energy required to deform the polymer, the reactant cavity will be treated as a sphere, and the transition state neck will be taken as a cylinder. Further discussion is provided below.

There are a number of other factors that have been ignored either because they are assumed to be small or because they are difficult to quantify. First, the penetrant might be able to move some distance within the cavity, an assumption which could break down for very small penetrants or for very large cavities. Second, the model assumes that the cavities remain relatively fixed in space during the course of the jump. However, once the penetrant has squeezed past the neck atoms into the product cavity, the neck atoms might be pushed into the reactant cavity where there is now empty space. The penetrant has not jumped past the whole width of the neck atoms but only a small part of it. The simulations do suggest a trend: if the penetrant in either the reactant or product cavity is already partially squashed, then the jump length is shorter.

Models for Critical Energy for the Average Jump. E_0 is the difference between the energy minima of the reactant and transition state. We need to pick out the key components of E_0 or somehow average over all the contributing degrees of freedom.

E_{def} is defined as the change in the energy of the polymer in going from reactant to transition state, so named because E_{def} consists of changes in energy due to deformation of the polymer: bends, torsions and nonbonded Lennard−Jones interactions between polymer atoms. E_{LJ} is defined as the remainder, the energy for the penetrant to squeeze through the neck, arising from changes in Lennard−Jones interactions between the penetrant and polymer atoms. The simulations show that both contributions to the minimum energy path are important, as seen in Table 1, with E_{def} on average about two-thirds of E_0 and E_{LJ} about one-third. Figure 3 shows how these energies vary along the reaction coordinate for a jump. Note that the reaction coordinate is highly tortuous, and it follows many small motions of many atoms: it is not a simple line joining the two cavity centers.

In order to find E_0 we need the potential energy functions for the reactant and transition states, since E_0 is the difference in energy between the minima of these functions. We define the four potential functions $V_{def}^{TS}(r)$, $V_{def}^{RS}(r)$, $V_{LJ}^{TS}(r)$, and $V_{LJ}^{RS}(r)$. The superscript refers to reactant state or transition state, and when the superscript is omitted, the statement applies to both states. The subscript "def" means a potential for expanding the cavity or neck to radius r. The subscript "LJ" means the Lennard−Jones energy of the penetrant in a cavity or neck of radius r.

Models for Polymer Deformation Potential. Deforming the polymer is probably a cooperative process involving small contributions from many atoms to $V_{def}(r)$. We expect this to be a cooperative and not a short-range process because the simulations show that if one includes motions of a smaller sphere of polymer atoms around the penetrant, the E_0's are much higher. The present simulations and those reported elsewhere by Greenfield and Theodorou allow enough polymer atoms to move so that the value of E_0 seems to converge, although a more accurate test of this by allowing even more polymer atoms to move is not possible given the computational restrictions.

In virtually every jump from the simulations, polymer−polymer nonbonded interactions make a large positive contribution to E_{def}, as seen in Figure 3, while torsional and bending contributions fluctuate about zero, without any noticeable trend. This is further evidence that forming the neck is not the result of a few local bends or torsions. As an example, with typical bond-angle force constants, a bend of 10° requires ~5 kJ mol^{-1}. A few of these combined with a few other associated contributions would soon give an energy greater that the E_0 obtained from the simulations. Torsional contributions are likely to be small because of their high force constants.

To simplify the local polymer structure surrounding the neck, our model assumes that this structure can be averaged out and treated as an isotropic continuum with thermodynamic properties of the bulk. We are assuming that the use of a bulk property is like averaging over many jumps to find the property for a typical jump. The reasons above suggest that enough of the polymer is involved that this approximation is valid for neck formation and cavity expansion. We present two separate treatments for this bulk expression for V_{def}.

(a) Compressible-Fluid Model. The first bulk property used to model V_{def} is the isothermal compressibility κ. The work W to create a volume V against a given pressure p exerted by the polymer is given by

$$W = \int_{V_i}^{V} p(V')\, dV' \tag{5}$$

where V_i is the original volume. In this model, we treat the polymer as a continuum, whose total volume remains fixed as the neck opens. The reversible isothermal work for opening up a small cavity in a fluid under constant total volume, neglecting surface tension effects, is

$$W = p_i \Delta V + \frac{\Delta V^2}{2\kappa V} \tag{6}$$

where p_i is the initial pressure, ΔV is the change in volume of the cavity, V is the constant total volume, and κ is the isothermal compressibility. If the dominant term is the work in compressing the fluid (i.e., the term involving κ), then W depends only on the change in volume.[67] Treating the cavity as a sphere and the neck as a cylinder, the volume change is a concentric expansion from old radius r_i to new radius r. In addition it is necessary to specify the volume V in eq 4, which is defined by the distance beyond which the expansion has

no significant effect. We rather arbitrarily assume that the radius beyond which the polymer atoms are unaffected by the expansion is twice the radius of the cavity or neck. This leads to the following potentials for deforming the polymer:

$$V_{\mathrm{def}}{}^{\mathrm{RS}}(r) = \frac{2\pi(r^3 - (r_i{}^{\mathrm{RS}})^3)^3}{21\kappa(r_i{}^{\mathrm{RS}})^3} \tag{7}$$

$$V_{\mathrm{def}}{}^{\mathrm{TS}}(r) = \frac{L_{\mathrm{n}}\pi(r^3 - (r_i{}^{\mathrm{TS}})^3)^2}{14\kappa(r_i{}^{\mathrm{TS}})^3} \tag{8}$$

(b) The Linear Elastic Solid Model. In this model, we assume that microscopically the polymer behaves like a linear elastic solid with the same material constants as the macroscopic solid. For the transition state, we need to calculate the energy required to expand a cylindrical cavity in an elastic solid, and, for the reactant state, we need to calculate the energy to expand a spherical one. Both these problems may be solved with the theory of linear elasticity, which may be found in many texts.[68] We include details of these calculations in the appendix with this paper. A summary follows here.

The strain energy of a linear elastic solid is given by

$$U = \int \frac{1}{2} e_i{}^j \tau_i{}^j \, \mathrm{d}V \tag{9}$$

where the Einstein summation convention has been used, the integration is over the whole volume of the polymer, $e_i{}^j$ is the strain tensor and $\tau_i{}^j$ is the stress tensor. Physically, this expression is a sum over the whole polymer of the work required to deform each element of volume. It is this U that will give us V_{def} for deformation to a given r. U can be thought of as the Helmholtz free energy relative to the relaxed polymer at the same temperature.

We assume that the vector which gives the deformation of a point in the polymer initially at $\mathbf{r}$ is $\mathbf{u}(\mathbf{r}) = (u(r),0,0)$ in (r, θ, ϕ) coordinates. After calculating the stress and strain tensors in terms of $u(r)$, we have U as a functional of $u(r)$. The configuration that the polymer adopts for a given expansion of the cavity or neck will clearly be that which minimizes the energy U. The calculus of variations allows us to find the $u(r)$ which minimizes U in each state:

$$u^{\mathrm{RS}} = \frac{A}{r^2} \qquad u^{\mathrm{TS}} = \frac{B}{r} \tag{10}$$

where A and B are constants. Substituting this back into the expression for U gives the $V_{\mathrm{def}}(r)$ potentials

$$V_{\mathrm{def}}{}^{\mathrm{RS}} = 8\pi\mu \, r_i{}^{\mathrm{RS}}(r - r_i{}^{\mathrm{RS}})^2 \tag{11}$$

$$V_{\mathrm{def}}{}^{\mathrm{TS}} = 2\pi\mu \, L_{\mathrm{n}}(r - r_i{}^{\mathrm{TS}})^2 \tag{12}$$

where μ is one of the Lamé elastic constants, equal to the shear modulus of the polymer. It is defined as follows:

$$\mu = \frac{E}{2(1+\nu)} \tag{13}$$

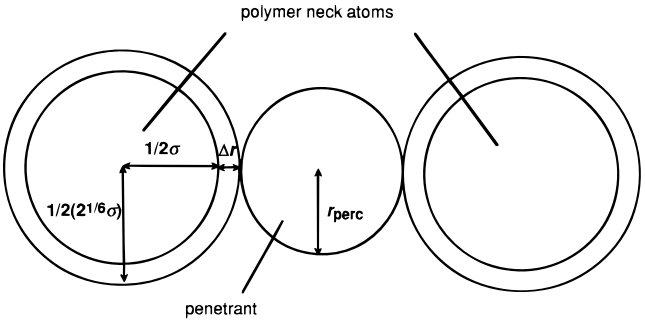

Figure 4. Illustration of how the percolation radius of the penetrant is increased by Δr when considering polymer atoms as having a radius of $^1/_2\sigma$.

where E is Young's modulus and ν is Poisson's ratio for the bulk polymer. Note also that Young's modulus, the isothermal compressibility, and Poisson's ratio are not independent, they obey $E = 3\kappa^{-1}(1 - 2\nu)$.

Model for Penetrant−Polymer Potential. The second potential function needed is $V_{\mathrm{LJ}}(r)$: the Lennard−Jones energy of the penetrant in a neck or cavity of radius r. Qualitatively, this is expected to be a monotonically decreasing function of distance until it becomes essentially zero for $r \geq \sigma/2$, where the small attractive component of the Lennard−Jones potential is unimportant in our calculations. The simulations show that the nonbonded interactions between penetrant and the closest polymer atoms in the reactant cavity can range from ∼0.7 to ∼2 kJ mol^{-1}. However, in the transition state, the penetrant has large repulsive interactions with three to four polymer neck groups, most of which are methyls. Such energies are consistent with the geometry of our model described above. We therefore take the two Lennard−Jones potentials to be of the form

$$V_{\mathrm{LJ}}(r) = 4n\epsilon\left[\left(\frac{\sigma}{r'}\right)^{12} - \left(\frac{\sigma}{r'}\right)^{6}\right] \tag{14}$$

where n is 3 for the transition state and 4 for the reactant state, and the Lennard−Jones parameters are those between penetrant and surrounding groups, and

$$r' = r + {}^1/_2\sigma(\text{side group}) \tag{15}$$

is the distance between side group and penetrant atoms, as seen in Figure 4, and σ and ϵ are obtained using the standard combining rules for Lennard−Jones interactions between different groups. For an interaction between two species A and B, the Lennard−Jones parameters are given by

$$\sigma = {}^1/_2(\sigma_{\mathrm{A}} + \sigma_{\mathrm{B}}) \qquad \epsilon = \sqrt{\epsilon_{\mathrm{A}}\epsilon_{\mathrm{B}}} \tag{16}$$

The overall potentials $V^{RS}(r)$ or $V^{TS}(r)$ are given by the sum of V_{def} and V_{LJ}, and the difference in the minima of each of these with respect to distance of these gives the activation energy

$$E_0 = \min(V^{TS}) - \min(V^{RS}) \tag{17}$$

where $V^{\mathrm{TS}} = V_{\mathrm{def}}{}^{\mathrm{TS}} + V_{\mathrm{LJ}}{}^{\mathrm{TS}}$ and $V^{\mathrm{RS}} = V_{\mathrm{def}}{}^{\mathrm{RS}} + V_{\mathrm{LJ}}{}^{\mathrm{RS}}$ are the total potentials for the two states. Figures 5 and 6 show $V^{RS}(r)$ and $V^{TS}(r)$ for both models, with parameter values as specified in Table 2 for polypropyl-

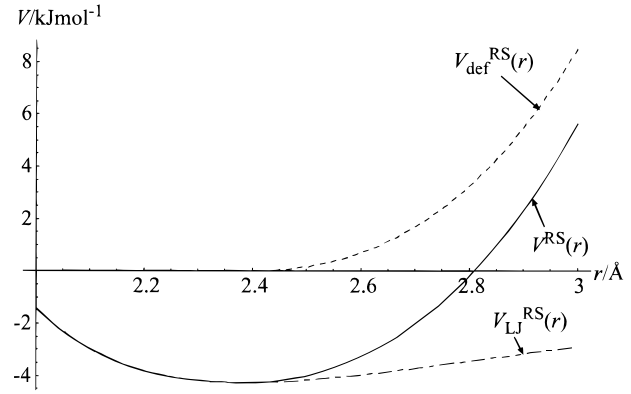

Figure 5. Various potential functions in the reactant state in the LES model, for polypropylene. The parameters are given in Table 2.

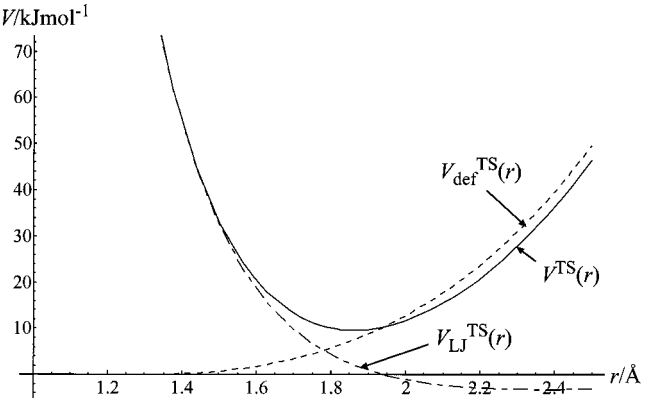

Figure 6. Various potential functions in the transition state in the LES model, for polypropylene. The parameters are given in Table 2.

Table 2. Bulk Properties,[70] Lennard−Jones Parameters,[72] and Geometrical Parameters Used in the Calculation of the Diffusion Coefficient of Methane in Atactic Polypropylene at 233 K

$T = 233$ K
$\kappa = 2.94 \times 10^{-10}$ Pa^{-1}
$E = 2.65 \times 10^{9}$ Pa
$\nu = 0.37$
$\mu = 0.97 \times 10^{9}$ Pa
$\sigma_{methyl} = 3.56$ Å
$\epsilon_{methyl} = 70$ K
$r_i^{TS} = 1.1$ Å
r_i^{RS}-CF model = 1.6 Å
r_i^{RS}-LES model = 2.5 Å

ene. It is informative to see how E_0 varies with penetrant size, which can be achieved by varying the Lennard−Jones diameter. The result is shown in Figure 7, where the diameters are chosen to correspond to a range of different penetrants (see below). The curve is not smooth because the Lennard−Jones well depth and penetrant mass both vary independently as the penetrant size increases.

Model for $Q^{\dagger}/Q$. $Q^{\dagger}/Q$ is the ratio of the partition function of the transition state to that of the reactant state. In general, a partition function in a unimolecular reaction is made up of components for rotational, translational, vibrational, and hindered-rotor modes. A polymer system only has the last two of these. What level of detail does one need for the various vibrations and hindered rotations? Clearly these modes are many in number. Figure 8 shows the distribution function of the frequencies of the modes in the simulation, obtained by the usual normal-mode analysis. The distribution of frequencies in the transition state closely resembles

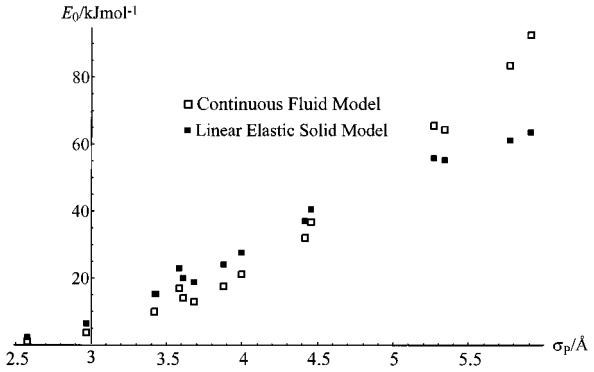

Figure 7. Calculated variation of the critical energy with penetrant diameter for PVC at 298 K, as predicted by the two models: compressible fluid and linear elastic solid. The variation with diameter is not smooth because the mass and Lennard−Jones well depth of the penetrants also vary in these calculations. The penetrants are in order of increasing size, He, H_2, Ar, O_2, MeOH, Kr, N_2, CH_4, CO_2, C_2H_6, EtOH, C_6H_6, n-C_4H_{10}, n-C_5H_{10}, and n-$C_6 10_{14}$, with values for σ and ϵ from ref 72. The other parameters are as in Table 3.

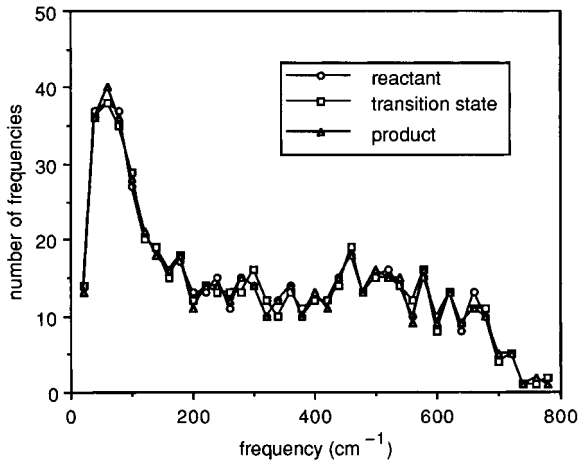

Figure 8. Number distribution of reactant, transition-state, and product frequencies for jump 4 in the simulations (see Table 1). The frequencies were grouped into 20 cm^{-1} bins to obtain this distribution.

that of the reactant state, although individual frequencies might vary significantly. This implies that the jumping event has no major "global" effect on the polymer modes.

The similarity of the frequency distributions is important since equation 1 shows that it is the *ratio* of partition functions that is important. If the reactant and transition-state frequency distributions of Figure 8 were identical, then $Q^{\dagger}/Q = 1$. The most primitive approximation is then to assume that there is no difference between Q and $Q^{\dagger}$, in which case the frequency factor A is approximately given by $k_B T/h \sim 10^{13}$ s^{-1}. We can do better than this, although it does show that the *maximum* value of the frequency factor for k_{jump} is $\sim 10^{13}$ s^{-1}. In fact $Q^{\dagger}/Q < 1$ because the transition state has one degree of freedom less than the reactant state. The simulation data for $Q^{\dagger}/Q$ in Table 1 give values significantly less than unity.

The expression for the partition function for a quantum mechanical harmonic oscillator of frequency f is

$$q_{vib} = \frac{1}{1 - e^{-hf/k_B T}} \tag{18}$$

(which refers to the zero-point energy as "energy =

zero"), showing that an individual component of Q and $Q^\dagger$ is only significantly different from unity when hf becomes comparable to k_BT, i.e. for $f < 500\ \mathrm{cm}^{-1}$. Figure 8 shows that there are many such modes. Even for higher frequencies, the accumulated product of many individual ratios which differ from unity by only a small amount can be itself very different from unity.

In conventional applications of unimolecular reaction theory to gas-phase reactions, it is common to develop semiempirical models based on differences between normal modes of reactant and transition state.[19] The dot products of the displacement vectors defining the normal modes give some information on this question for the present polymer system. The closer this dot product is to unity, the more the two modes resemble each other. This is another way of gauging the change in the nature of the motion in going from reactant to transition state. Evaluation of the dot products between all pairs of the normal modes of Figure 8 shows that the largest dot products are always between modes of similar frequencies. While many reactant modes are similar to one of the transition-state modes (with a dot product between 0.5 and 1), others show extensive coupling.

Additional information can also be obtained from the participation ratios.[69] These indicate the fraction of all atoms in the system participating in a particular normal mode, and therefore give information about the delocalization in that mode. Most modes show variable delocalization, with participation ratios in the range 0.08−0.3. Interestingly, the reaction coordinate has a very low participation ratio: 0.0016. Since there are about 900 atoms in the simulation, this implies that about 1.4 atoms participate effectively in this mode; obviously, the most important of these is the penetrant. Clearly there is scope for further work to develop a knowledge of the distribution function for lower frequencies for reactant and transition-state modes in an glassy polymer.

Calculation of $Q^\dagger/Q$. We assume that (as suggested by Figure 8) there are only a few modes which are important in determining $Q^\dagger/Q$. There are three components of these differences, one due to penetrant's internal motions, q_{pe}, one due to polymer deformations, q_{def}, and one due to the motion of the penetrant in the Lennard−Jones field of the polymer, q_{LJ}:

$$\frac{Q^\dagger}{Q} = \frac{q_{pe}{}^\dagger q_{LJ}{}^\dagger q_{def}{}^\dagger}{q_{pe} q_{LJ} q_{def}} \tag{19}$$

Since the penetrant is treated as a united atom, it has no internal degrees of freedom, and so $q_{pe} = q_{pe}{}^\dagger$. The partition functions q_{LJ} and $q_{LJ}{}^\dagger$ are included as the translational motions of the penetrant in the harmonic approximation to the Lennard−Jones field of the polymer. The Lennard−Jones potential field is a sum of potentials, one for each neighboring polymer side group. Each term in this sum is given by

$$V_{LJ}(r) = 4\epsilon\left[\left(\frac{\sigma}{|\mathbf{r} - \mathbf{r}_{sg}|}\right)^{12} - \left(\frac{\sigma}{|\mathbf{r} - \mathbf{r}_{sg}|}\right)^{6}\right] \tag{20}$$

where $\mathbf{r}_{sg}$ is the location of the side group. As described above, the transition state has three side groups arranged trigonally and the reactant state has four, arranged tetrahedrally. Given this Lennard−Jones potential for the position of the penetrant $\mathbf{r}$, the force constants in the harmonic approximation are the second derivatives of the potential function at its minimum.

The side groups which form the cavity or neck can be allowed to move while maintaining the tetrahedral or trigonal symmetry, so that the radius of the cavity or neck varies. The radius, which already appears in the above potentials in $\mathbf{r}_{sg}$, is then another degree of freedom which can be included in the partition function using normal mode analysis and the harmonic approximation. The extra degree of freedom is constrained by the deformation potential so including it does not significantly alter the results, and the side groups were held fixed.

There are two degrees of freedom for penetrant motion in the transition state and three for the reactant state, so there are two force constants for the transition state and three for the reactant state. Given the force constants and the mass of the penetrant, each frequency is given by

$$f = \frac{1}{2\pi}\sqrt{\frac{m}{k}} \tag{21}$$

where k is the force constant. Then the partition function is given by eq 18.

While $q_{po}{}^\dagger/q_{po}$ is expected to be slightly less than 1, since the polymer will be more constrained in the transition state, we approximate it as unity.

Diffusion coefficients may now be found. The rate coefficient is given by the transition state theory formula, eq 1. E_0 in this equation is given by eq 17 with potentials given by eqs 7, 8, 11, 12, and 14. The partition function for each degree of freedom of the penetrants motion is given by eq 18, with the frequency given by eq 21 and the force constant from the potential in eq 20. Once the rate coefficient has been found, eq 3 gives the jump length and eq 2 gives the diffusion coefficient.

Results

We compare our model to the simulation data on polypropylene used in the development of the model and to experimental data on poly(vinyl chloride). Unfortunately, no satisfactory experimental data on polypropylene are available.

Comparison with Simulations on Polypropylene. The parameters used for polypropylene[70] are shown in Table 2. Greenfield and Theodorou's simulations[3] show that onset of percolation in the polymer structure occurs for penetrants of radius 0.9 Å. Thus there is an accessible volume cluster for such a penetrant, the so-called infinite cluster, that stretches across the entire simulation cube. We take the radius of this penetrant as r_i^{TS}, the radius of the transition state neck in the absence of the penetrant. Penetrants with the percolation radius therefore do not require a deformation of the polymer to fit through the neck. We need to use $2^{1/6}\sigma/2$ as the penetrant radius. The difference in radius Δr, between a methyl group of radius $^1/_2(2^{1/6}\sigma)$ and one of radius $^1/_2\sigma$ is

$$\Delta r = {}^1/_2\sigma(2^{1/6} - 1) \tag{22}$$

which has a value ∼0.2 Å for the present system. Figure 4 illustrates this modification. This suggests that a penetrant of radius 0.9 + 0.2 = 1.1 Å can percolate the structure, where polymer and penetrant atoms are now treated as hard spheres with radius $^1/_2\sigma$-

Table 3. Bulk Properties,[71] Lennard−Jones Parameters,[72] and Geometrical Parameters Used in the Calculation of the Diffusion Coefficient of Various Penetrants in Atactic Poly(vinyl chloride) at 298 K[a]

$T = 298$ K
$\kappa = 2.65 \times 10^{-10}$ Pa^{-1}
$E = 2.6 \times 10^{9}$ Pa
$\nu = 0.385$
$\mu = 0.94 \times 10^{9}$ Pa
$\sigma_{Cl} = 3.4$ Å
$\epsilon_{Cl} = 120$ K
r_i^{TS}-CF model = 1.0 Å
r_i^{TS}-LES model = 0.5 Å
r_i^{RS}-CF model = 1.6 Å
r_i^{RS}-LES model = 2.5 Å

[a] See Figure 9 for comparison of theory with experiment.

(CH_3). Hence, r_i^{TS} is taken as 1.1 Å. In general:

$$r_i^{TS} = r_{perc} + \Delta r = r_{perc} + {}^1/_2(2^{1/6} - 1)\,\sigma(\text{side group}) \tag{23}$$

For the linear elastic model we took r_i^{RS}, the radius of the reactant cavity in the absence of the penetrant, as 2.5 Å, which is the same value obtained below by fitting theory to experiment for poly(vinyl chloride). A diffusion coefficient of 2.22×10^{-9} cm^2 s^{-1} is obtained along with the critical energy $E_0 = 19.1$ kJ mol^{-1} and $Q^\dagger/Q = 0.014$. These results are typical of the jumps found by computer simulation by Greenfield and Theodorou (see Table 1). For the continuous fluid model r_i^{RS} was taken as 1.6 Å, and this gives a diffusion coefficient of 1.43×10^{-7} cm^2 s^{-1} with $E_0 = 16.35$ kJ mol^{-1} and $Q^\dagger/Q = 0.09$, which are also consistent with the simulation data. Unfortunately, full stochastic simulations on the polypropylene system have not yet been performed, and so it is not possible to compare the result from our typical jump model with a single diffusion coefficient from a proper stochastically-averaged series of simulations.

Comparison with Experiments on Poly(vinyl chloride). The bulk properties and parameters for poly(vinyl chloride) at 298 K are given in Table 3.[71] The diffusion coefficient was calculated for a series of species, He, H_2, Ar, O_2, MeOH, Kr, N_2, CH_4, CO_2, C_2H_6, EtOH, C_6H_6, n-C_4H_{10}, n-C_5H_{10}, and n-C_610_{14}, for which Lennard−Jones parameters are available.[72] Comparisons of the calculated values with some experimental data[73] for both models are given in Figure 9. Both the continuous fluid (CF) and linear elastic solid (LES) models reproduce the variation of diffusion coefficient with penetrant diameter. The curves of best fit indicate general trends, but these plots hide variations in ϵ and mass and so the fluctuations are expected. The only parameter used to fit the model to the experimental data was the radius of the reactant cavity in the absence of the penetrant, r_i^{RS}.

The results are insensitive to the radius of the transition state neck with no penetrant, r_i^{TS}. It is approximately 1 Å because we find 1.1 Å for the similar polymer polypropylene, and the results of our calculations depend only weakly on r_i^{TS} itself, but strongly on $r_i^{TS} - r_i^{RS}$. Since its deformation potential is much shallower, the LES model allows the neck to expand more for the same amount of energy. It is therefore logical to choose r_i^{TS} smaller for the LES model than for the CF model. Values of 0.5 Å for the LES model and 1.0 Å for the CF model were therefore used for r_i^{TS}. These choices are somewhat arbitrary, but do not significantly affect the results, and are satisfactory given that we cannot estimate r_i^{TS} as for polypropylene for lack of appropriate simulation data. Of course, r_i^{TS} could be used as another fitting parameter, but the fit to experiment is already good.

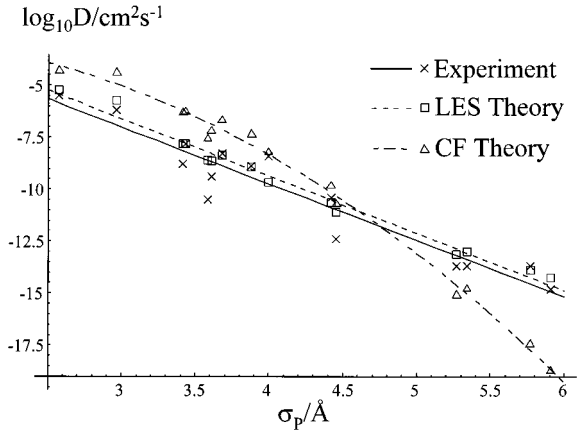

Figure 9. Comparison of the two models with experimental[73] diffusion coefficients for various penetrants in PVC at 298 K. Parameters for the calculation are given in Table 3. The penetrants are those listed under Figure 7, with values for σ and ϵ from ref 72. The radius of the transition state neck in the absence of the penetrant was chosen as 1 Å for the CF model and 0.5 Å for the LES model.

Given that r_i^{TS} is now fixed, and the sensitivity of the results to $r_i^{TS} - r_i^{RS}$, we choose to treat r_i^{RS} as an adjustable parameter. For the LES model $r_i^{RS} = 2.5$ Å gave the best agreement with the experiments. The agreement is better than Figure 9 indicates given that all the points for which the theoretical predictions are bad are either the noble gases or alcohols. It is promising that the chemical nature of the species affects the fit to the experiment. The different types of penetrant molecules will interact with the polymer differently, and a force law other than the simple Lennard−Jones potential may be needed. In other words the force between the penetrant and the polymer cannot be completely characterized by the two parameters σ and ϵ. Different values of r_i^{RS} are also needed because this number contains information about the shape and typical conformations of the penetrant.

Most of the species in the above list are hydrocarbons, and so our value of r_i^{RS} is typical of their interaction with the polymer. The polarity of the alcohols and the simple spherical shape of the noble gases mean their interaction with the polymer is very different. Hydrocarbons are quite flexible molecules and r_i^{RS} contains information about their conformation, since we assume a spherical penetrant.

This model would be very useful for extrapolating from experimental data on a few molecules to predict the diffusion coefficients of similar species at various temperatures. Figure 9 shows that even diffusion coefficients of quite different molecules are consistent with the one value of r_i^{RS}.

The continuous fluid model also reproduces the experimental data well, except for the two or three largest penetrants. The predicted diffusion coefficient for this model curves downwards at high penetrant diameters. This is because the potential for deforming the polymer is so steep that for larger penetrants the transition state becomes high in energy. The trend in E_0 with penetrant diameter is shown for both models in Figure 7, and this effect can be clearly seen.

The continuous fluid model would also be useful for predicting unknown diffusion coefficients but it would be safer to interpolate these rather than extrapolate.

Since the one value for the radius r_i^{RS} reproduces a whole range of diffusion coefficients, it must have some physical significance. The value of this radius which best fits the data is different for the two models, but that is because the different assumptions about the nature of the polymer lead to different effective cavity sizes. Thus the radius of the reactant cavity is a typical cavity size given our assumptions about the nature of the polymer. The value of our model lies in the ease with which these diffusion coefficients were calculated, each taking a few seconds on an ordinary personal computer; in fact, the calculations could be performed by hand. The consistency of the data for a single value of r_i^{RS} suggests that given r_i^{RS} found from a few experimental diffusion coefficients, the diffusion coefficients of many other species could be predicted.

Temperature Dependence of the Diffusion Coefficient. The temperature dependence of D predicted by the model is basically Arrhenius, with the pre-exponential T and $Q^{\dagger}/Q$ slowly varying with respect to temperature relative to the exponential. Fitting to predicted diffusion coefficients between 100 K and 400 K gives an activation energy of 23.5 kJ mol^{-1}, and a frequency factor of $10^{10.8}$ s^{-1}. This suggests that the value of E_0 should be a good approximation to the actual activation energy for diffusion. It is difficult to make a comparison with experiment because of the high uncertainty in literature data. For example, results[18] for diffusion of a tracer dye (TTI, which has quite a large size) in a glassy matrix (polystyrene with 10% tricresyl phosphate) suggest an activation energy on the order of 100 kJ mol^{-1}. However, the experimental data themselves are subject to very high uncertainty,[18] because of the small temperature range and the observation that the samples showed physical aging (the samples were not in equilibrium). Wachi and Yates[74] report temperature dependences for diffusion coefficients in poly(vinyl chloride), but with the activation energy greater above T_g than below. This reported result is surprising, and it is not clear that we can compare their results with our predictions meaningfully. One aspect of temperature dependence that the model has not taken into consideration is any change in polymer structure with temperature. How this affects the necks and cavities could be important, but is unknown.

Conclusions

A model for the diffusion coefficients of penetrants in a glassy polymer matrix has been developed based on simple semiempirical transition-state theory and simulation data. We feel that the treatment captures the essential physical process which dominates diffusion in a glassy polymer, that is with the penetrant occasionally jumping between cavities through a neck. The parameters in both models are readily evaluated from bulk properties of the polymer such as the isothermal compressibility, or the Young's modulus and Poisson's ratio. Both of the models reproduce the experimental trends. In general, one expects that such continuum mechanics-type approaches will underestimate the work required to form a neck, since there is a sacrifice in cohesive forces of the polymer in opening up such a small cavity. In an elementary way, this could be dealt with by introducing a surface tension times change in area term, a possible direction for the future.

Our model is useful both because it provides physical understanding and because it allows a few experimental diffusion coefficients to be used for extrapolation to predict many others.

Acknowledgment. The support of the Australian Research Council is gratefully acknowledged by A.A.G.W., R.H.H., and R.G.G. M.L.G. and D.N.T. thank the BF Goodrich Co. and Union Carbide for financial support.

Appendix—Linear Elastic Theory

Throughout the following cylindrical polar coordinates (r, θ, z), will be used. These coordinates are those which we apply to the transition state. All the following calculations may be reworked in spherical polars for the reactant state. We describe the deformation of the solid with the vector $\mathbf{u}(\mathbf{r}) = (u, v, w)$ which gives the displacement of the point which starts at $\mathbf{r}$ before the deformation. The local stretching, compression and shearing of an element of volume of the solid is given by the strain tensor $\mathbf{e}$. It is defined as the symmetric part of the dyad (outer product) $\nabla\mathbf{u}$,

$$\mathbf{e} = {}^1/_2(\nabla\mathbf{u} + (\nabla\mathbf{u})^T)$$

Such a definition of $\mathbf{e}$ assumes $\mathbf{u} \ll \mathbf{r}$ because ∇ is defined at $\mathbf{r}$, so the particle must be close to $\mathbf{r}$ or ∇ will have to be defined at $\mathbf{u} + \mathbf{r}$, which is the true location of the particle. This tensor gives us all the information we need about the solid, but we want to calculate $\mathbf{u}$ (which will give us the radius of the transition state neck); we therefore write $\mathbf{e}$ in terms of $\mathbf{u}$. It is simpler to exploit the cylindrical symmetry of the transition state and take $\partial_z = 0$ and $w = 0$. This says that we are dealing with an expansion of the tube which does not vary along its length, and that there is no deformation in the z direction (plane strain).

Finding $\mathbf{e}$ in terms of $\mathbf{u}$

$$\mathbf{e} = \frac{1}{2}\left[\left(\hat{\mathbf{r}}\frac{\partial}{\partial r} + \frac{\hat{\theta}}{r}\frac{\partial}{\partial\theta}\right)(\hat{\mathbf{r}}u + \hat{\theta}v) + \left(\left(\hat{\mathbf{r}}\frac{\partial}{\partial r} + \frac{\hat{\theta}}{r}\frac{\partial}{\partial\theta}\right)(\hat{\mathbf{r}}u + \hat{\theta}v)\right)^T\right]$$

$$= \hat{\mathbf{r}}\hat{\mathbf{r}}\frac{\partial u}{\partial r} + (\hat{\mathbf{r}}\hat{\theta} + \hat{\theta}\hat{\mathbf{r}})\left(\frac{1}{r}\frac{\partial u}{\partial\theta} + \frac{\partial v}{\partial r} - \frac{v}{r}\right) + \hat{\theta}\hat{\theta}\frac{1}{r}\left(\frac{\partial v}{\partial\theta} + u\right)$$

For our purposes $v = 0$, because a given point in the polymer moves only radially outward from the penetrant. Also by symmetry, u does not vary with θ. So finally

$$\mathbf{e} = \hat{\mathbf{r}}\hat{\mathbf{r}}\frac{\partial u}{\partial r} + \theta\theta\frac{u}{r}$$

The above calculations can also be carried through with the more elegant but more difficult index notation using the Einstein summation convention. We start from the metric tensor

$$g_{rr} = 1, \quad g_{\theta\theta} = r^2, \quad g_{zz} = 1$$

with all other elements zero, and the definition

$$e_i^j = \frac{1}{2}\left(\frac{\partial u^i}{\partial x^j} + \frac{\partial u^j}{\partial x^i}\right)$$

where taking the symmetric part of $\partial u^i/\partial x^j$ explicitly eliminates rotations. The results from this calculation agree with those obtained above in the index-free notation

$$e_r^r = \frac{\partial u^r}{\partial r}, \qquad e_\theta^\theta = \frac{u^r}{r}$$

with all other elements zero.

We now define the stress tensor, which gives the force across any element of area on any imaginary or real surface inside the solid. Put mathematically

$$\mathrm{d}\mathbf{F} = \tau \cdot \mathrm{d}\mathbf{S}$$

where d**S** is a vector element of area, d**F** is the force across the element of area, and τ is the stress tensor.

The stress and strain tensors in an isotropic elastic solid are related as follows:

$$\tau_i^j = \lambda e_i^j \delta_i^j + 2\mu e_i^j$$

λ and μ are the Lamé elastic constants, a set of material constants equivalent to Young's modulus and Poisson's ratio. This equation is the 3-dimensional analogue of $F = -kx$. Only μ is important for our results, and it is defined

$$\mu = \frac{E}{2(1+\nu)}$$

We now need to find equations for the deformation of the polymer. The energy of an element of volume in a deformed linear elastic solid is given by

$$\mathrm{d}U = {}^1/_2 e_i^j \tau_i^j \mathrm{d}V$$

This result may be derived by considering the work done in deforming the solid. It is really just the 3-dimensional analog of $\mathrm{d}U = \mathrm{d}w = F \cdot \mathrm{d}x$ (no heat flow). U can be thought of as the Helmholtz free energy relative to the relaxed polymer at the same temperature. Clearly the configuration the solid adopts will be that which minimizes the internal energy, so

$$U = \int {}^1/_2 e_i^j \tau_i^j \, \mathrm{d}V$$

will be a minimum and

$$\delta \int {}^1/_2 e_i^j \tau_i^j \mathrm{d}V = 0$$

$$\delta \int {}^1/_2 e_i^j (\lambda e_k{}^k \delta_i^j + 2\mu e_i^j) \, \mathrm{d}V = 0$$

$$\delta \int {}^1/_2 \lambda (e_k{}^k)^2 + \mu e_i^j e_i^j \, \mathrm{d}V = 0$$

where the stress−strain relations have been taken from above and δ denotes a first-order variation of the integral. Substituting for the various components of e_i^j which were calculated above

$$\delta \int_{r_i}^{\infty} \frac{1}{2}\lambda \left(\frac{\partial u}{\partial r} + \frac{u}{r}\right)^2 + \mu \left[\left(\frac{\partial u}{\partial r}\right)^2 + \left(\frac{u}{r}\right)^2\right] 2\pi r L_n \, \mathrm{d}r = 0$$

where L_n is the length of the neck. This last line says that the total internal energy of the polymer (the elastic solid) is a minimum. The function $u(r)$ tells us how far a particle initially at r is displaced outward, and we have neglected all other displacements.

The function $u(r)$ which minimizes the above integral is a solution to the Euler−Lagrange equation

$$r^2 u''(r) + r u'(r) - u(r) = 0$$

which has the solution

$$u(r) = \frac{A}{r} + Br$$

Clearly $B = 0$ because the deformation cannot diverge at infinity.

We can now find $u(r)$:

$$u(r_i) = u_i$$

$$u(r) = \frac{u_i r_i^{\,2}}{r}$$

This last result can be substituted back into the integral for the internal energy, which finally gives us our V_def, the energy required to expand the transition state neck by u_i,

$$V_{\mathrm{def}}{}^{\mathrm{TS}} = 2\pi\mu \, L_\mathrm{n} u(r_i)^2$$

$$= 2\pi\mu \, L_\mathrm{n} (r - r_i)^2$$

and the same method for the spherical symmetry of the reactant state gives

$$V_{\mathrm{def}}{}^{\mathrm{RS}} = 8\pi\mu \, r_i \, u(r_i)^2$$

$$= 8\pi\mu \, r_i (r - r_i)^2$$

References and Notes

(1) Stannet, V.; Crank, J.; Park, G. S. *Diffusion in Polymers*; Academic: New York, 1968.
(2) Gilbert, R. G. *Emulsion Polymerization: A Mechanistic Approach*; Academic: London, 1995.
(3) Greenfield, M. L.; Theodorou, D. N. *Macromolecules* **1993**, *26*, 5461.
(4) Greenfield, M. L.; Theodorou, D. N. *Proc. Am. Chem. Soc. Div. Polym. Mater. Sci. Eng. (PMSE)* **1994**, *71*, 407.
(5) Greenfield, M. L.; Theodorou, D. N. *Polym. Prepr. (Am. Chem. Soc.)* **1995**, *36*, 687.
(6) Greenfield, M. L. Molecular Modeling of Dilute Penetrant Gas Diffusion in a Glassy Polymer using Multidimensional Transition-State Theory. Ph.D. Thesis: University of California, Berkeley, 1996.
(7) Pant, P. V. K.; Boyd, R. H. *Macromolecules* **1993**, *26*, 679.
(8) Rigby, D.; Roe, R. J. *J. Chem. Phys.* **1987**, *87*, 7285.
(9) Rigby, D.; Roe, R. J. *Macromolecules* **1990**, *23*, 5312.
(10) Roe, R. J. *Adv. Polym. Sci.* **1994**, *116*, 111.
(11) Takeuchi, H.; Roe, R.-J. *J. Chem. Phys.* **1991**, *94*, 7458.
(12) Barrer, R. M. *Nature* **1937**, *140*, 106.
(13) Barrer, R. M. *Trans. Faraday Soc.* **1939**, *35*, 629.
(14) Barrer, R. M. *Trans. Faraday Soc.* **1939**, *35*, 644.
(15) Takeuchi, H. *J. Chem. Phys.* **1990**, *93*, 2062.
(16) Sok, R. M.; Berendsen, H. J. C.; van Gunsteren, W. F. *J. Chem. Phys.* **1992**, *96*, 4699.
(17) Müller-Plathe, F.; Laaksonen, L.; van Gunsteren, W. F. *J. Mol. Graphics* **1993**, *11*, 118.
(18) Ehlich, D.; Sillescu, H. *Macromolecules* **1990**, *23*, 1600.
(19) Gilbert, R. G.; Smith, S. C. *Theory of Unimolecular and Recombination Reactions*; Blackwell Scientific: Oxford, England, and Cambridge, MA, 1990.
(20) Geisel, T.; Zacherl, A.; Radons, G. *Z. Phys. B* **1988**, *71*, 117.
(21) Chernikov, A.; Petrovichev, B.; Rogalsky, A.; Sagdeev, R.; Zaslavsku, G. *Phys. Lett. A* **1990**, *144*, 127.
(22) Chaikovsky, D.; Zaslavsky, G. *Chaos* **1991**, *1*, 463.
(23) Klafter, J.; G. Z. *Phys. Rev. E* **1994**, *49*, 4873.
(24) Stern, S. A.; Frisch, H. L. *Ann. Rev. Mater. Sci.* **1981**, *11*, 523.
(25) Fujita, H. *Fortschr. Hochpolym.-Forsch.* **1961**, *3*, 1.
(26) Vrentas, J. S.; Duda, J. L. *J. Polym. Sci., Polym. Phys. Ed.* **1977**, *15*, 403.
(27) Vrentas, J. S.; Duda, J. L. *J. Polym. Sci., Polym. Phys. Ed.* **1977**, *15*, 417.
(28) Vrentas, J. S.; Duda, J. L. *J. Polym. Sci., Polym. Phys. Ed.* **1977**, *15*, 441.
(29) Vrentas, J. S.; Vrentas, C. M. *Macromolecules* **1993**, *26*, 1277.
(30) Vrentas, J. S.; Vrentas, C. M. *Macromolecules* **1994**, *27*, 5570.

(31) Vrentas, J. S.; Vrentas, C. M.; Faridi, N. *Macromolecules* **1996**, *29*, 3272.
(32) Brandt, W. W. *J. Phys. Chem.* **1959**, *63*, 1080.
(33) DiBenedetto, A. T. *J. Polym. Sci.* **1963**, *A1*, 3477.
(34) Pace, R. J.; Datyner, A. *J. Polym. Sci., Polym. Phys. Ed.* **1979**, *17*, 437.
(35) Pace, R. J.; Datyner, A. *J. Polym. Sci., Polym. Phys. Ed.* **1979**, *17*, 453.
(36) Pace, R. J.; Datyner, A. *J. Polym. Sci., Polym. Phys. Ed.* **1979**, *17*, 465.
(37) Jagodic, F.; Borstnik, B.; Azman, A. *Makromol. Chem.* **1973**, *173*, 221.
(38) Gusev, A. A.; Arizzi, S.; Suter, U. W. *J. Chem. Phys.* **1993**, *99*, 2221.
(39) Gusev, A. A.; Suter, U. W. *J. Chem. Phys.* **1993**, *99*, 2228.
(40) Gusev, A. A.; Müller-Plathe, F.; van Gunsteren, W. F.; Suter, U. W. *Adv. Polym. Sci.* **1994**, *116*, 207.
(41) Baker, J. *J. Comput. Chem.* **1986**, *7*, 385.
(42) June, R. L.; Bell, A. T.; Theodorou, D. N. *J. Phys. Chem.* **1991**, *95*, 8866.
(43) Takeuchi, H. *J. Chem. Phys.* **1990**, *93*, 4490.
(44) Takeuchi, H.; Okazaki, K. *J. Chem. Phys.* **1990**, *92*, 5643.
(45) Takeuchi, H.; Roe, R.; Mark, J. E. *J. Chem. Phys.* **1990**, *93*, 9042.
(46) Takeuchi, H.; Roe, R.-J. *J. Chem. Phys.* **1991**, *94*, 7446.
(47) Takeuchi, H.; Okazaki, K. *Makromol. Chem., Macromol. Symp.* **1993**, *65*, 81.
(48) Müller-Plathe, F. *J. Chem. Phys.* **1991**, *94*, 3192.
(49) Müller-Plathe, F.; Rogers, S. C.; van Gunsteren, W. F. *Macromolecules* **1992**, *25*, 6722.
(50) Müller-Plathe, F.; Rogers, S. C.; van Gunsteren, W. F. *J. Chem. Phys.* **1993**, *98*, 9895.
(51) Pant, P. V. K.; Boyd, R. H. *Macromolecules* **1991**, *24*, 6325.
(52) Pant, P. V. K.; Boyd, R. H. *Macromolecules* **1992**, *25*, 494.
(53) Tamai, Y.; Tanaka, H.; Nakanishi, K. *Macromolecules* **1994**, *27*, 4498.
(54) Sonnenburg, J.; Gao, J.; Weiner, J. H. *Macromolecules* **1990**, *23*, 4653.
(55) Müller-Plathe, F. *J. Chem. Phys.* **1992**, *96*, 3200.
(56) Chassapis, C. S.; Petrou, J. K.; Petropoulos, J. H.; Theodorou, D. N. *Macromolecules* **1996**, *29*, 3615.
(57) Gee, R. H.; Boyd, R. H. *Polymer* **1995**, *36*, 1435.
(58) Smit, E.; Mulder, M. H. V.; Smolders, C. A.; Karrenbeld, H.; van Eerden, J.; Feil, D. *J. Membr. Sci.* **1992**, *73*, 247.
(59) Zhang, R.; Mattice, W. L. *J. Membr. Sci.* **1995**, *108*, 15.
(60) Takeuchi, H.; Okazaki, K. *Mol. Simul.* **1996**, *16*, 59.
(61) Theodorou, D. N.; Suter, U. W. *Macromolecules* **1985**, *18*, 1467.
(62) Go, N.; Scheraga, H. A. *Macromolecules* **1976**, *9*, 535.
(63) Tanemura, M.; Ogawa, T.; Ogita, N. *J. Comput. Phys.* **1983**, *51*, 191.
(64) Arizzi, S.; Mott, P. H.; Suter, U. W. *J. Polym. Sci., Polym. Phys. Ed.* **1992**, *30*, 415.
(65) Greenfield, M. L.; Theodorou, D. N. *Mol. Simul.* **1997**, in press.
(66) Arizzi, S. Diffusion of small molecules in polymeric glasses: a modelling approach. Ph.D. Thesis: M. I. T., 1990.
(67) Lipscomb, G. G. *AIChE J.* **1990**, *36*, 1505.
(68) Popov, E. P. *Engineering mechanics of solids*; Prentice-Hall: Princeton, NJ, 1990.
(69) Bell, R. J.; Dean, P.; Hibbins-Buttler, D. C. *J. Phys. C.: Solid State Phys.* **1970**, *3*, 2111.
(70) Theodorou, D. N.; Suter, U. W. *Macromolecules* **1986**, *19*, 139.
(71) Bicerano, J. *Prediction of polymer properties*; 2nd ed.; Marcel Dekker: New York, 1996.
(72) Hirschfelder, J. O.; Curtiss, C. F.; Bird, R. B. *Molecular Theory of Gases and Liquids*; Wiley: New York, 1964.
(73) Koros, W. J.; Fleming, G. K.; Jordan, S. M.; Kim, T. H.; Hoehn, H. H. *Prog. Polym. Sci.* **1988**, *13*, 339.
(74) Wachi, S.; Yates, J. G. *J. Polym. Sci., Polym. Phys. Ed.* **1991**, *29*, 1069.

MA970349F